International Academy of Science,
Engineering and Technology
Connecting Researchers; Nurturing Innovations

IASET

THE IMPROVED ROLLING BALL MODEL (IRBM) FOR LIGHTNING PROTECTION SYSTEM

EMECHEBE JONAS N[1], OTAVBORUO ERICSSON E[2], NZEAKO A. N[3] & ANI C. I[4]

[1]Federal Radio Corporation of Nigeria, Abuja, Nigeria

[2,4]Department of Electronic Engineering, UNN, Nsukka, Nigeria

[3]Department of Electrical and Electronic Engineering, CRUTECH, Calabar, Nigeria

ABSTRACTs

This paper describes a method for improving the Rolling Ball Model (RBM) of a Lightning Protection System (LPS). The RBM applies a single vertical air terminal and a down conductor which shunt lightning current to the ground. This Model has a limitation; it could give a protection only up to 45.7m height as against the height of 100m and above for a typical radio broadcasting tower in Nigeria. The introduction of two horizontal rods to the vertical rod of the RBM improves the protection potential of the Lightning Protection System (LPS). This method is called the Improved Rolling Ball Method (IRBM). The IRBM is implemented with data from the physical specifications of the two horizontal rods, the height of the tower, the electric field strength and the rate of change of the electric field strength.

KEYWORDS: Horizontal rods, IRBM, LPS, Nigeria, RBM

INTRODUCTION

An atmospheric lightning is one of nature's most spectacular phenomena which has fascinated and frightened man throughout the times. When it passes over a region, it is attracted or discharged to hills, trees, towers, masts, buildings etc. [1, 2]. Disruption of service may occur during lightning discharge. Earlier works theorized the causes and consequences of lightning current, its origin and the mechanism responsible for its buildup. Currently, disciplines in engineering and sciences are primarily focused on how to design a lightning protection system, which can capture lightning discharge. The application of a single vertical air terminal and a down conductor which shunts lightning to the ground, otherwise known as the Rolling Ball Model (RBM), is very popular [3, 4, 5]. The concept of this model (RBM) is based on the principle of mathematical geometry. But, the single air terminal has a limitation. Between 100-300m, the RBM is ineffective and unreliable in protecting a radio equipment against horizontal flashes [5]. This informs the introduction of two horizontal rods to the existing vertical rods to improve the protection potential of the Lightning Protection System (LPS). This technique is known as the Improved Rolling Ball Method (IRBM). The IRBM is very effective in protecting the radio equipment from lightning current. By implication, the horizontal rods prevent the rolling ball from making contact with the device mounted in between the rods.

LIGHTNING CHARACTERISTICS

The study of lightning characteristics such as the electromagnetic field and radiation, leader currents, return strokes and their relationships are very important in the modeling a of telecommunication towers with a radio system mounted on it. A number of measurements and theoretical investigation of lightning discharge are based on the

electro-geometric and improved electro-geometric models (EGM and IEGM) [6, 7]. The relationship between the electromagnetic field radiation and the return stroke of EGM and IEGM are developed by employing the theory of mathematical geometry. Thus a critical review of the literature provides the background for developing an accurate predictive model. Previous models [1] assume that the return stroke current initiates from the ground surface. However, for tall structures such as telecommunication and transmission line towers, the return stroke current is initiated near the point of discharge [6,7]. Previous models also assume that the return stroke current distributes uniformly along the lightning path and the tall structure with reflection from the ground. Such models are not suitable in principle for the analysis of the electromagnetic fields of lightning to tall structures because the electromagnetic fields depend on the propagation and the distribution of the lightning current inside the lightning discharge, and the tall structure.

Lightning discharge involves both the movement and neutralization of charge volumes. A cloud discharge affects both negative and positive regions of a dipole. The discharge results in an electric field change in which the magnitude and direction depend on the location of the point at which measurement is taken [8]. Lightning discharges include cloud-cloud, intra-cloud, cloud-air, known as atmospheric discharges, and cloud-ground. Suggestion for suitable conditions for measurement of atmospheric electricity is to collect data either above or on the surface of the earth [9]. It is a common practice in atmospheric electricity to assume that lightning discharged to the ground neutralizes a single spherically symmetric cloud charge distribution [10]. It has been argued that under certain specific conditions the discharge within the cloud was initiated by a positive streamer from the center of the upper positive region (P-region) moving downwards to the center of the Lower negative region (N-region) [4].

Other works [3, 4, 5, 10] opine that, within the cloud (intra-cloud), the charge could also be initiated by an N-region moving towards a P-region. The intra-cloud discharge accounts for the majority of all lightning discharges. Although the magnitude varies, it may also cause damage to a device in the lower atmosphere-the troposphere. The atmosphere is divided into four layers. The layers are: the troposphere and tropopause, the stratosphere and the stratopause, the mesosphere and mesopause and the thermosphere. The troposphere is the closest to the ground and it extends to about 16 km above the earth. It is the layer where human lives and jets fly [11]. The stratosphere is the next layer to the troposphere and it extends to about 50km. It is followed by the mesosphere and then finally the thermosphere. The tower lies in the troposphere; specifically 155m above the ground [11, 12, 13]. Analysis of the work covers up to 200m of the bottom of the troposphere. Several other works argued that atmospheric lightning is based on the principles of charge mechanisms. Some of the popular mechanisms are contact electrification; electromechanical charging; polarization; influence charging; diffusion charging and mechanisms involving freezing and splinting of ice particles.

The thunderclouds are the atmospheric engine that produces the lightning discharges. It is the cause of the atmospheric instability and formation of atmospheric convection [1, 3]. How thundercloud becomes electric charge is subject to arguments to the scientists and engineers [3, 9]. Some researchers argued that ionization of the atmosphere is caused majorly by the continual cosmic rays which emanate from the sun flare. This is also responsible for the formation of lightning and corona process.

CONTACT MECHANISM

Contact or Volta electrification involves mechanical contact between solids where electrons flow from a metal of lower work function over to another metal of a higher work function. Contact potential comes about when solid particles bounce off the material surface on the ground or in the troposphere [1, 14].

ELECTROCHEMICAL MECHANISM

Any processes in which charges are captured or transferred by ions in the troposphere are referred to as electrochemical process. Continual ionization of existing ionic particles in the presence of strong electric field intensity over a long distance could result in the generation of lightning current [15]. When the process of ionization by collision is confined to a small volume and electric field force near a point, point discharge occurs. For example, falling water drops can acquire a negative charge if the positive ions move more slowly in a normal positive potential gradient [2].

PRECIPITATION MECHANISM

All forms of moisture too heavy to remain suspended in the air fall to the ground. This is known as precipitation. Generally the process of charge separation in the atmosphere is based on water drops and ice particles from snow, hail or rain precipitation. Thunderstorm generation, separation and discharge of electronic charges (positive and negative charges) based on the precipitation process has been regarded as the only dominant mechanism responsible for the buildup of the high electric field which causes a lightning flash [16, 17 18, 19].

POLARIZATION MECHANISM

Polarization is defined as the result of the collision and separation of particles velocities in the presence of an ambient electric field [20]. Cloud containing large ice particles and small drops is found to be the most favourable for the growth of the electric field intensity, which produce lightning current. Lightning is produced mostly by a glaciated cloud within an infinitesimal period, compared to warm cloud which seldom produces lightning [20, 21].

EVAPORATION AND CONDENSATION MECHANISM

The evaporation and condensation mechanism (ECM) is another process under which the generation of charges in the atmospheric troposphere. It proposes positive atmospheric electrification of liquid drops during evaporation and negative electrification during condensation of liquid drops. Thundercloud is based on the gravitational, aerodynamic and electrical forces produced by condensation and evaporation [16, 22].

This work aims at modeling the cloud-to ground lightning discharge. It is conceptualized by the mathematical geometric projection which is illustrated in Figure (2a) and (2b).

THE IMPROVED ROLLING BALL MODEL (IRBM)

The geometric projection of the IRBM structure in Figure 1 is illustrated in Figure 2a-b. Figure 2a-b comprises the heights of the upper and lower rods (H and h), the horizontal reference points (B and O) from H and h, and the horizontal distance (D) between the tower and the reference points (B and O). The path lengths R_1 and R_2 are the directions of the field intensities with angles α_1 and α_2 from points B and O.
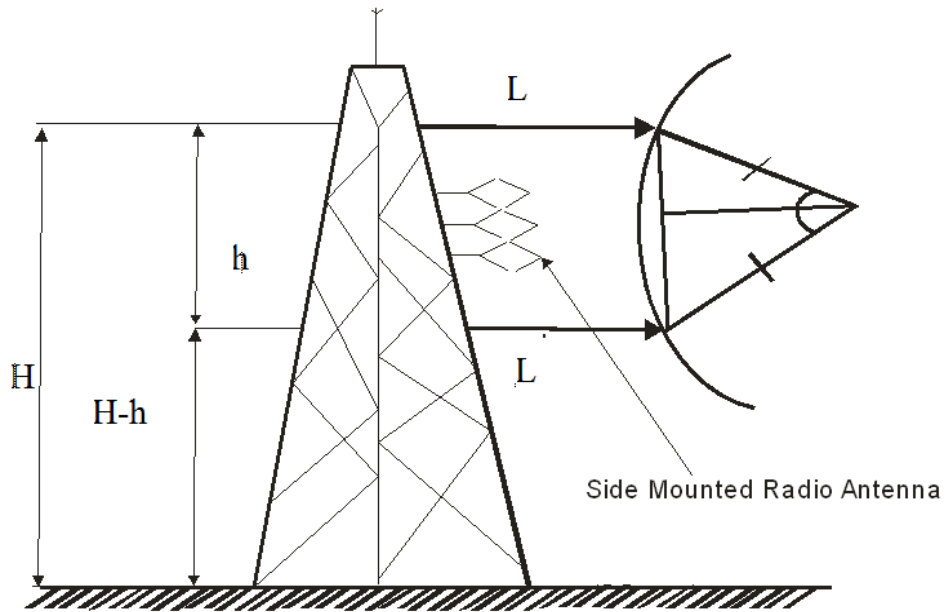
Figure 1: Architecture of the IRBM

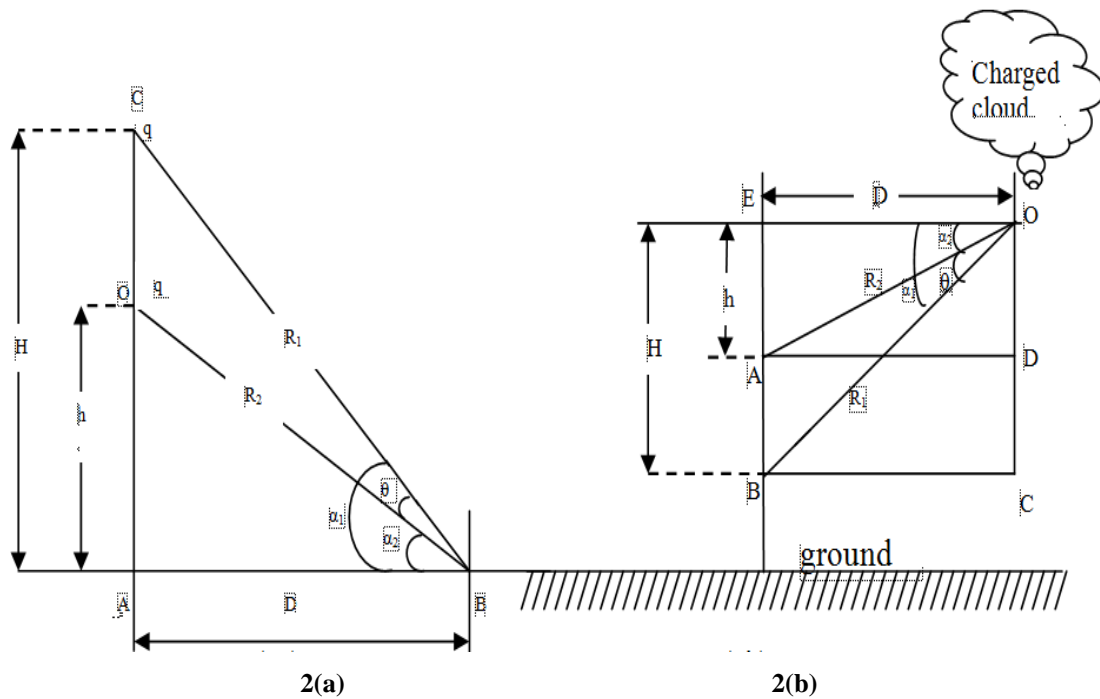2(a)   2(b)

Figure 2: Geometric Projection of the IRBM with Two Horizontal Rods

From Δ ABC and Δ ABO, the geometric dimensions of figure 2a are determined as follows:

$$Sin\,\alpha_1 = \frac{CA}{CB} = \frac{H}{R_1}, \; Cos\,\alpha_1 = \frac{AB}{CB} = \frac{D}{R_1}, \; R_1 = \left(H^2 + D^2\right)^{\frac{1}{2}} \quad - \qquad - \tag{1}$$

$$Sin\,\alpha_2 = \frac{h}{R_2}, \; Cos\,\alpha_2 = \frac{D}{R_2}, \; R_2 = \left(h^2 + D^2\right)^{\frac{1}{2}} \quad - \qquad - \qquad - \qquad - \tag{2}$$

Similarly, from Δ OEB and Δ OEA, the geometric dimensions of figure 2b are determined as follows:

$$\sin \alpha_1 = \frac{BE}{BO} = \frac{H}{R_1}, \cos \alpha_1 = \frac{OE}{OB} = \frac{D}{R_1}, R_1 = \left(H^2 + D^2\right)^{1/2} \qquad - \qquad - \qquad - \tag{3}$$

$$\sin \alpha_2 = \frac{AE}{OA} = \frac{h}{R_2}, \cos \alpha_2 = \frac{OE}{OA} = \frac{D}{R_2}, R_2 = \left(h^2 + D^2\right)^{1/2} \qquad - \qquad - \qquad - \tag{4}$$

Correspondingly, the electric field strength of the upper horizontal rod (E_u) along hypotenuse CB or OB is expressed in equation (5). The E_u is a function of the charge, the air medium constant, length of the of the hypotenuse, and the sine of the angle. Clearly, Figure 2b is a mirror image of Figure 2a.

$$E_u = E_1 * \sin \alpha_1 = \frac{QkH}{R_1^3} \qquad - \qquad - \qquad - \qquad - \qquad - \qquad - \qquad - \tag{5}$$

Where,

$$E_1 = \frac{Qk}{R_1^2}$$

$$k = \frac{1}{4\pi\varepsilon_0}$$

R_1 = distance between C and B

By substituting equation (1) into equation (5), the electric field strength of the upper horizontal rod becomes equation (6).

$$E_u = QkH * \frac{1}{\left(H^2 + D^2\right)^{\frac{3}{2}}} \qquad - \qquad - \qquad - \qquad - \qquad - \qquad - \qquad - \tag{6}$$

Correspondingly, the electric field strength of the lower horizontal rod (E_L) with respect to the point B is illustrated by equation (7).

$$E_L = \frac{Qkh}{R_2^3} = Qkh * \frac{1}{\left(h^2 + D^2\right)^{\frac{3}{2}}} \qquad - \qquad - \qquad - \qquad - \qquad - \tag{7}$$

The electric field strength between the upper and the lower horizontal rods (E_{uL}) is presented in equation (8).

$$E_{UL} = E_U - E_L = QkH * \frac{1}{\left(H^2 + D^2\right)^{\frac{3}{2}}} - Qkh * \frac{1}{\left(h^2 + D^2\right)^{\frac{3}{2}}} \qquad - \qquad - \qquad - \tag{8}$$

The derivative of the electric field of the horizontal rods, shown in equations (6 & 7), with respect to time is formulated. The change in electric field with time is expressed as a function of lightning current (i), H, h, and D as shown in equations (9 & 10).

$$\frac{dE_U}{dt} = \frac{Hk}{\left(H^2 + D^2\right)^{\frac{3}{2}}} \frac{dQ}{dt} = \frac{Hki}{\left(H^2 + D^2\right)^{\frac{3}{2}}} \qquad - \qquad - \qquad - \qquad - \qquad - \qquad (9)$$

$$\frac{dE_L}{dt} = \frac{hki}{\left(h^2 + D^2\right)^{\frac{3}{2}}} \qquad - \qquad - \qquad - \qquad - \qquad - \qquad - \qquad - \qquad - \qquad (10)$$

By substituting the expression of the lightning current (*i*) presented in a research paper [6], the change in the electric field of the IRBM is illustrated by equation (11-12).

$$\frac{dE_U}{dt} = \frac{Hk}{\left(H^2 + D^2\right)^{\frac{3}{2}}} \left(\frac{I_p}{\eta} * \frac{1}{1 + \left(\frac{t}{\tau_2}\right)^c} * \frac{\frac{1}{m!}\left(\frac{t}{\tau_1}\right)^m}{1 + \sum_{i=1}^{\infty} \frac{1}{m!}\left(\frac{t}{\tau_1}\right)^m} \right) \qquad - \qquad - \qquad - \qquad (11)$$

$$\frac{dE_L}{dt} = \frac{hk}{\left(h^2 + D^2\right)^{\frac{3}{2}}} \left(\frac{I_p}{\eta} * \frac{1}{1 + \left(\frac{t}{\tau_2}\right)^c} * \frac{\frac{1}{m!}\left(\frac{t}{\tau_1}\right)^m}{1 + \sum_{i=1}^{\infty} \frac{1}{m!}\left(\frac{t}{\tau_1}\right)^m} \right) \qquad - \qquad - \qquad - \qquad (12)$$

By making Ip the subject of the expression in equation (12), the peak current becomes the formula in equation (13)

$$I_p = \frac{dE_L}{dt} \frac{\left(h^2 + D^2\right)^{\frac{3}{2}}}{hk} \eta * \left(1 + \left(\frac{t}{\tau_2}\right)^c \right) * \frac{1 + \sum_{i=1}^{\infty} \frac{1}{m!}\left(\frac{t}{\tau_1}\right)^m}{\frac{1}{m!}\left(\frac{t}{\tau_1}\right)^m} \qquad - \qquad - \qquad - \qquad (13)$$

METHODOLOGY

The mathematical model in equations (8), (11) and (12) are simulated. The simulation model is carried out with the Microsoft Excel 2007 spreadsheet. The model is run and statistical data is collected at the end of the simulation. The parameters used for simulating the electric field strength for varying horizontal distance (D), i.e equation (8) are: electric charge (Q) $=5*10^{-8}$C, air medium (k)= 1.0006, permittivity of free space (εo) = $8.85*10^{-12}$ F/m, Height of the tower (H_T) = 50-200m, D=0-50, height of the lower rod (h)=41.8m. Figures (3a) and (3b) illustrate the graph of field strength against horizontal distance. In addition, the parameters for simulating the electric field between the rods, i.e equations (11)-(12), are: εo = $8.85*10^{-12}$ F/m, H_T = 75m, k=1.0006, D= 0-50, Q=5-20C. The parameters for simulating the rate of change of the electric field strength between the rods are: H_T=50-200m, D= 0-270m, Q = $5*10^{-8}$C, εo = $8.85*10^{-12}$ F/m, k=1.0006. Figure (4a) and (4b) are the outcome of the simulation. Similarly, the electric field and the rate of change of electric field strength illustrated in Figures (5a) and (5b) are simulated with the following parameters: H_T=150m, Q = $5*10^{-8}$C, εo = $8.85*10^{-12}$ F/m, k=1.0006, distance between the upper and lower horizontal rods (H-h)= 2.6 – 31.2m,

D= 0 – 9 m.

RESULTS AND DISCUSSIONS

Figure 3a-b describes the electric field strength experienced by the upper and lower horizontal rods which protects the radio equipment. The measurement of the electric field strength decreases with the increase in the distance between the tower and the reference point for specified values of the upper and lower horizontal rods respectively. The drop in the slope of the electric field strength is steep when the charge = 20C and gentle at 5C in Figure 3.

With the upper horizontal rod (H) = 75m and horizontal distance = 0 - 50m, the electric field strength decreases from: $3.56*10^{-3}$ $-2.05*10^{-3}$, $2.67*10^{-3}$- $1.54*10^{-3}$, $1.78*10^{-3}$ – $1.02*10^{-3}$ and $8.89*10^{-4}$ – $5.12*10^{-4}$ V/m for specified charge (Q) = 20 C, 15C, 10C, and 5C, respectively. Similarly with the lower horizontal rod = 41.8m and the horizontal distance = 0-50m and the same magnitudes of charges, the field strengths are: $1.15*10^{-2}$ – $3.02*10^{-3}$, $8.59*10^{-3}$ – $2.27*10^{-3}$, $5.73*10^{-3}$ – $1.51*10^{-3}$, $2.86*10^{-3}$ – $7.56*10^{-4}$, respectively.
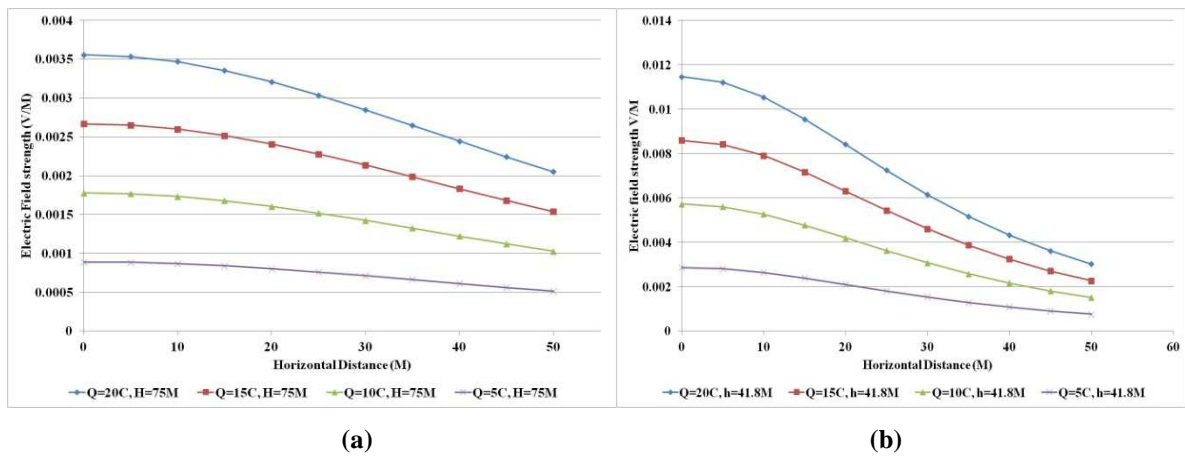

(a)   **(b)**

Figure 3(a): Electric Field Strength vs. Horizontal Distance for Specified Magnitude of Charges (Q); (b) Electric Field Strength vs. Horizontal Distance for Specified Magnitude of

Figure 4a-b gives a description of the electric field strengths and the rate of change of the electric field strengths with respect to time for varying height of the tower from the ground, respectively. In Figure 4a, the electric field strength drops with the variation in the height (H_T) of the tower from 50 -200m. At Q = $5*10^{-8}$C, (H_T)= 50-110m, and specified horizontal distance (D) = 0-20m, the field strength drop steeply. But, between 110–250m, the drop in electric field strength is very gentle, and all the electric field strengths converged as illustrated in Figure (4a). The drop in the field strengths are; $2*10^{-11}$-$1.25*10^{-12}$, $1.97*10^{-11}$-$1.25*10^{-12}$, $1.89*10^{-11}$-$1.25*10^{-12}$, $1.76*10^{-11}$-$1.24*10^{-12}$, and $1.60*10^{-11}$-$1.23*10^{-12}$V/m when D=0-20m, respectively, at H=110-250m.

In Figure 4b, the rate of change of electric field (dE/dt) decreases with increase in (H_T) at D=0-60m. At (H_T)=50-200m, dE/dt=$7.39*10^{-6}$-$5.4*10^{-7}$, $4.66*10^{-6}$-$4.06*10^{-7}$, and $1.94*10^{-6}$ – $3.50*10^{-7}$ V/ms when D = 0-60m, respectively. The measurement of dE/dt increases and then drops continually with increase in heights (H_T) from 50-200m at specified values of D -D= 90-150m- as illustrated in Figure 4b. At D=180-270, the measurement of dE/dt increases exponentially with increase in (H_T). The range of dE/dt =$1.42*10^{-7}$-$1.90*10^{-7}$, $9.19*10^{-8}$-$1.52*10^{-7}$, $6.27*10^{-8}$-$1.21*10^{-7}$, and $4.02*10^{-8}$-$9.07*10^{-8}$ at D=180-270m, respectively.

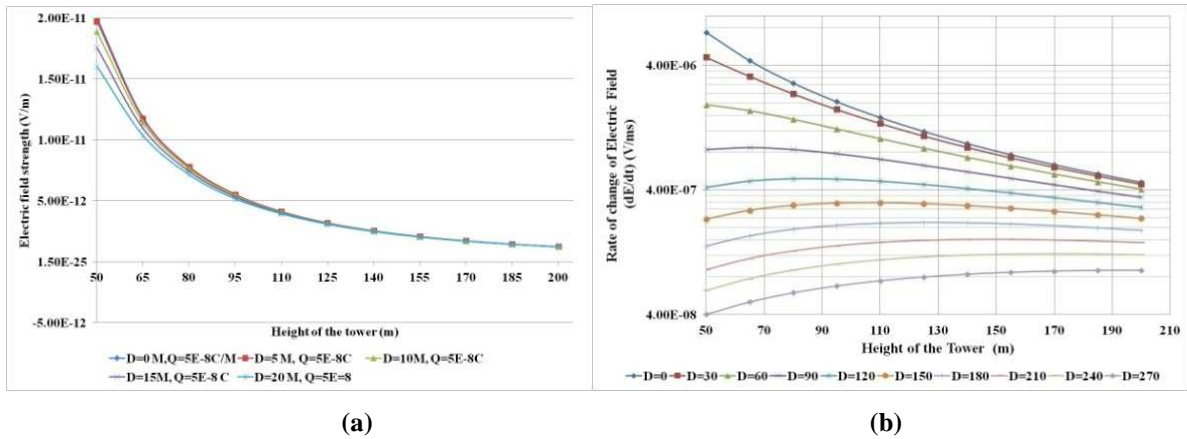(a)   (b)

Figure 4(a): Electric field Strength vs. Height of the Tower(H_T); (b) Rate of Change of Electric Field vs. Height of the Tower(H_T)

The behaviour of the electric field strength (E) and the rate of change of the electric field strength (dE/dt) between the horizontal rods (D_{Hh}) at D=0-9m are captured by Figure 5a- b. At D =0-5m, the electrtic field (E) and the rate of electric field (dE/dt) decrease acutely with increase in the separation between the rods. The field strengths (Es) at D=0-5m and D_{Hh} = 2.6-32.6m are: $7.40*10^{-9}$-$5.14*10^{-11}$, $2.08*10^{-9}$-$5.07*10^{-11}$, $7.27*10^{-10}$-$4.95*10^{-11}$ while dEs/dt = $2.73*10^{-3}$-$1.90*10^{-5}$, $7.68*10^{-4}$-$1.87*10^{-5}$, $2.69*10^{-4}$-$1.83*10^{-5,}$ respectively. However, a surge in E and dE/dt occur between D_{Hh} 2.6-7.6m. A surge is also known as a spike; it is the surge which damage radio equipment when a vertical air terminal is applied. On the contrary, it is arrested by one of the horizontal rods shown in Figure 2. The electric field strength increases from $3.12*10^{-10}$ to $3.92*10^{-10}$ and then drop continuously and exponentially to $4.77*10^{-11}$ at D=5 and D_{Hh}= 7-9m. Similarly, at D=7m and D_{Hh}=7-9m, E increases from $1.58*10^{-10}$ to $2.32*10^{-10}$ and then decreases exponentially to $4.56*10^{-11}$. Under the same condition, dE/dt increases from $1.15*10^{-4}$-$1.25*10^{-3}$, $5.85*10^{-5}$-$8.53*10^{-5}$ and later decreases to $1.76*10^{-5}$ and $1.68*10^{-5}$, correspondingly.

(a)   (b)
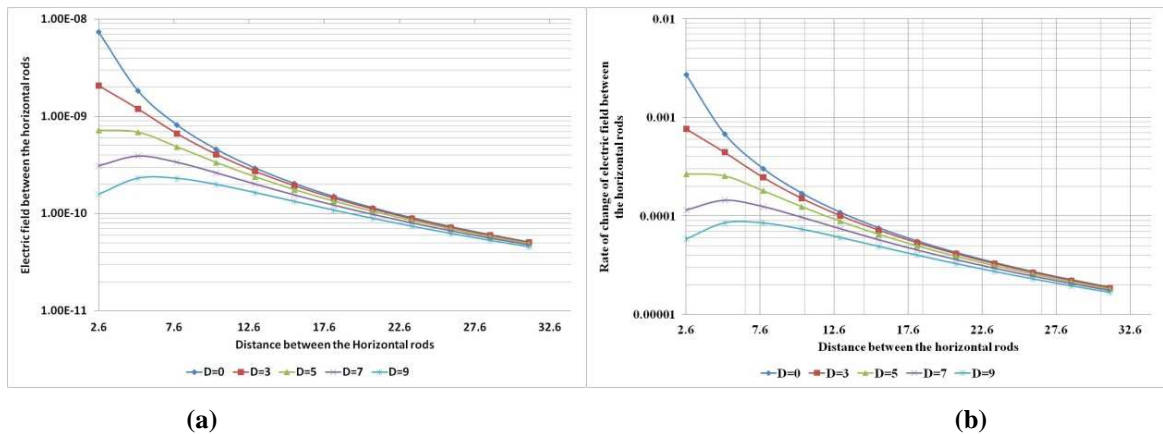
Figure 5(a): Electric Field Strength (E) vs Distance Between the Horizontal Rods; (b) Rate of Change of Electric Field Strength (dE/dt) vs Distance Between the Horizontal Rods

CONCLUSIONS

The measurement of the electric field strength of the IRBM model decreases with the increase in the distance between the tower and the reference point as illustrated in the geometric projection in Figure 2a-b. The drop in the slope of

the electric field strength is steep when the charge = 20C and small at 5C as illustrated in Figure 3. In Figure 4a, the electric field strength drops with the variation in the height (H_T) of the tower from 50 -200m. At Q = $5*10^{-8}$C, (H_T)= 50-110m, and specified horizontal distance (D) = 0-20m, the field strength drop steeply. However, between 110–250m, the drop in electric field strength is small, and all the electric field strengths converge. Furthermore, in Figure 4b, the rate of change of electric field (dE/dt) decreases with increase in (H_T) at D=0-60m. The measurement of dE/dt increases and then drops continually with increase in (H_T) from 50-200m at specified values of D-D= 90-150m. Finally, at D=180-270, the measurement of dE/dt increases exponentially with increase in (H_T). The electric field strengths fluctuate rapidly and then decrease with increase in the separation between the horizontal rods.

From the results illustrated in Figure 4b it could be deduced that the rate at which lightning discharge is captured by the horizontal rods depends on the polarity of the parallel rods. For instance, a positive upper rod attracts a negative lightning discharge while the negative lower rod attracts the positive lightning discharge. By implication, Figures 5a-b clearly demonstrate charge neutralization between the horizontal rods when lightning occurs around the region. The RBM, which applies a single rod captures only the vertical lightning strikes while the two horizontal rods in the IRBM model capture the horizontal lightning strikes which bypass the vertical rod projected by the RBM model. Lightning strike is discharged downward when the distance between the horizontal rods (D_{Hh}) = 7.6-32.6m as shown in Figure 5. The improvement which the IRBM has over the RBM technique is the presence of the uniform field which is created between the horizontal rods. This field creates an electromagnetic potential difference (Pd) between the rods, which accelerates the discharge of the horizontal lightning current through the downward conductor to the earth. In addition, the positioning of the two horizontal rods enhanced the protective capacity of the RBM; the RBM can only protect a digital equipment up to a height of 45.7m on the tower. But, the IRBM can protect the same device up to a height of 100m and above. Furthermore, the geometric properties, such as the distance between the two horizontal rods (D_{Hh}), the radius and the cross sectional area of the rods, are used in calibrating the electric field and the rate of change of the electric in the IRBM. The result of this calibration is an improved protection potential of the Lightning Protection System (LPS).

REFERENCES

1. Matoyama H. et al, "Electromagnetic Field Radiation Model for Lightning Strokes to Tall Structures," IEEE trans. power delivery, vol. 11, no. 3, July 1996, pp. 1624-1632.

2. Malan D. J, "Physics of Lightning," The English University Press, London, 1963, pp. 1-176.

3. Uman M. A, "The Arts and Science of Lightning Protection," Cambridge University Press, Cambridge, 2008, pp. 1-240.

4. Khastgir S. R and Saha S. K, "On Intra-cloud Discharges and their accompanying Electric Field Changes," J. of Atmos. Terr. Phys., vol. 33, Jan. 1972, pp. 115-126.

5. Ogawa T and Brook M, "The mechanism of the Intracloud lightning," J. Geophysical Res. Vol 69, no. 24, 1964 pp. 5141-5150.

6. Emechebe J. N, et al, "Lightning Protection System: A Comparative Analysis of four Modified Models," J. IJECE, vol. 2, 1ss. 5, Nov. 2013.

7. Emechebe J. N et al, "Comparative Analysis of Original and Modified Lightning Protection Systems," J. IJECE, vol. 3, Iss. 2, Mar. 2014.

8. Harris D. J and Salman Y. E, "The Measurement of Lightning Characteristics in Northern Nigeria," J. of Atmos. Terr. Phys., vol. 34, Jan. 1972, pp. 775-786.

9. Chalmer s J. A, "The Measurement of the vertical Electric Current in the Atmosphere, J. of Atmos. Terr. Phys., vol. 24, Jan. 1962, pp. 297-302.

10. Jacobson E. A and Krider E. P, "Electrostatic Field Changes Produced by Florida Lightning," J. of Atmos. err. Phys., vol. 33, no. 1, Jan. 1976, pp. 103-117.

11. "The Vertical profile of our Atmosphere," http://www.starhop.com/library/pdf/studyguide/elementary/brsp-4Layers.pdf.

12. "Layers of the Atmosphere," http://cindispace.utdallas.edu/education/atmosphere_info.pdf.

13. "The Habitable Planet," http://www.learner.org/courses/envsci/unit/pdfs/unit2.pdf.

14. Loeb L. B, "Experimental Contribution to the Knowledge of Charge Generation," in Byers H (ed.), Thunderstorm Electricity, Chicago press, Chicago, 1956, pp. 150-192.

15. Chalmers J. A., "Atmospheric Electricity," (2nd) Pergamon press, Oxford, 1967, pp. 1-515.

16. Kamra A. K, "The role of Electrical Forces in Charge Separation by Falling Precipitation in Thunderclouds," Journal of the Atmospheric Science, vol. 32, no. 1, 1975, pp. 143-157.

17. Workman E. J and Reynolds S. E, "Structure and Electrification," Thunderstorm Electricity, University of Chicago press, 1956, pp. 139-140.

18. Gunn R, "measurement of Electricity carried by Precipitation Particles," Thundercloud Electricity, ed. Byers pp. 193-206.

19. Chapman S, "Thundercloud Electrification in Relation to Rain and Snow Particles," Thundercloud Electricity, ed. Byers pp. 207-230.

20. Ziv A and Levin Z, "Thunder Electrification: Cloud Growth and Electrification Development," Journal of the Atmospheric Science, vol. 31, no. 6, Sept. 1974, pp. 1652-1661.

21. Mathur D, "Introduction," in Mathur D. (ed), "Ion Impact Phenomena," Springer, New York, 1991, pp. 1-11.

22. Kamra A. K and Vonnegut B, "A Laboratory Investigation of the Effect of Particle Collisions on the Generation of Electric Field in Thunderstorms," Journal of the Atmospheric Science, vol. 28, 1971, pp. 1182-1185.